JAIST Repository
https://dspace.jaist.ac.jp/

Title	In-plane isotropic magnetic and electrical properties of MnAs/InAs/GaAs(111)B hybrid structure
Author(s)	Islam, Md. Earul; Akabori, Masashi
Citation	Physica B: Condensed Matter, 532: 95-98
Issue Date	2017-03-06
Type	Journal Article
Text version	author
URL	http://hdl.handle.net/10119/15736
Rights	Copyright (C)2017, Elsevier. Licensed under the Creative Commons Attribution-NonCommercial-NoDerivatives 4.0 International license (CC BY-NC-ND 4.0). [http://creativecommons.org/licenses/by-nc-nd/4.0/] NOTICE: This is the author's version of a work accepted for publication by Elsevier. Md. Earul Islam and M. Akabori, Physica B: Condensed Matter, 532, 2017, 95-98, http://dx.doi.org/10.1016/j.physb.2017.03.013
Description	

JAIST
JAPAN
ADVANCED INSTITUTE OF
SCIENCE AND TECHNOLOGY

Japan Advanced Institute of Science and Technology

In-plane isotropic magnetic and electrical properties of MnAs/InAs/GaAs(111)B hybrid structure

*Md. Earul Islam and Masashi Akabori

Center for Nano Materials and Technology (CNMT), Japan Advanced Institute of Science and Technology (JAIST), 1-1 Asahidai, Nomi, Ishikawa 923-1292, JAPAN

E-mail: s1540002@jaist.ac.jp; akabori@jaist.ac.jp

*Corresponding author, e-mail: s1540002@jaist.ac.jp; Tel: +81-761-51-1920

Abstract

We characterized in-plane magnetic and electrical properties of MnAs/InAs/GaAs(111)B hybrid structure grown by molecular beam epitaxy (MBE). We observed isotropic easy magnetization in two crystallographic in-plane directions, $[\bar{2}110]$ and $[0\bar{1}10]$ of hexagonal MnAs i.e. $[\bar{1}10]$ and $[11\bar{2}]$ of cubic InAs. We also fabricated transmission line model (TLM) devices, and observed almost isotropic electrical properties in two crystallographic in-plane directions, $[\bar{1}10]$ and $[11\bar{2}]$ of cubic InAs. Also we tried to fabricate and characterize lateral spin-valve (LSV) devices from the hybrid structure. We could roughly estimate the spin injection efficiency and the spin diffusion length at room temperature in $[11\bar{2}]$ direction. We believe that the hybrid structures are helpful to design spintronic device with good flexibility in-plane.

Keywords

Molecular beam epitaxy (MBE); MnAs, InAs, GaAs(111)B; Magnetic properties; Transmission line model (TLM); Lateral spin-valve (LSV)

1. Introduction

In semiconductor spintronics, ferromagnetic/semiconductor hybrid structures have already attracted attention because of their potential application for spin field effect transistors (spin-FETs) [1]. For spin-FET application, it is necessary to have ferromagnetic source and drain for spin polarized carrier injection and detection, and semiconductor channel with spin-orbit coupling (SOC) controlled by electric field for spin polarized carrier transport. Hexagonal NiAs-type MnAs is a ferromagnetic metal with Curie temperature over room temperature [2], which can be synthesized with III-As semiconductors in epitaxial growth system [3]. III-As semiconductors are expected to show large SOC when the bandgap becomes narrow. InAs is a narrow bandgap III-As semiconductor. Therefore, MnAs/InAs hybrid structures with in-situ-formed interfaces are possible candidates for the base structures of spin-FET application. GaAs and InP are widely-used substrate materials for III-As as well as MnAs epitaxial growths. It is known that MnAs grown on GaAs (001) [4] sometimes shows mixed phase between hexagonal and orthorhombic structures, and also MnAs grown on GaAs(001) and InP(001)shows anisotropic in-plane magnetization [4, 5] where c-axis of hexagonal structure is in-plane-oriented to (001). On the other hand, on GaAs(111)B [6] or InP(111)B [7], only hexagonal NiAs-type MnAs with c-axis normal to the plane has been observed,

and has shown almost isotropic in-plane magnetization [8]. Moreover, considering spin-FET application, investigation of in-plane electrical properties is also important. However, there is no report on in-plane electrical properties using MnAs on (111)B, even though there are some reports on GaAs(001) [9] and InP(001) [10].

In this paper, we report on in-plane magnetic and electrical properties of a MnAs/InAs/GaAs(111)B hybrid structure grown by molecular beam epitaxy (MBE) for spin-FET application. Also we report on a trial of spin-valve measurements using the hybrid structure.

2. Sample preparation

We used semi-insulating GaAs(111)B substrates for MBE growth. The detail of MBE growth is discussed in elsewhere [11]. The MnAs/InAs was grown directly on the substrates without buffer layer. The nominal thicknesses of MnAs and InAs were ~200 nm and ~1.2 μm, respectively, as shown in Fig. 1. We confirmed good stacking of MnAs(0001)/InAs(111)B on GaAs(111)B and parallel alignment of MnAs $[\bar{2}110]$, InAs$[\bar{1}10]$, and GaAs $[\bar{1}10]$ by X-ray diffraction study [11]. After the growth, we removed indium metals on backside of the samples by polishing.

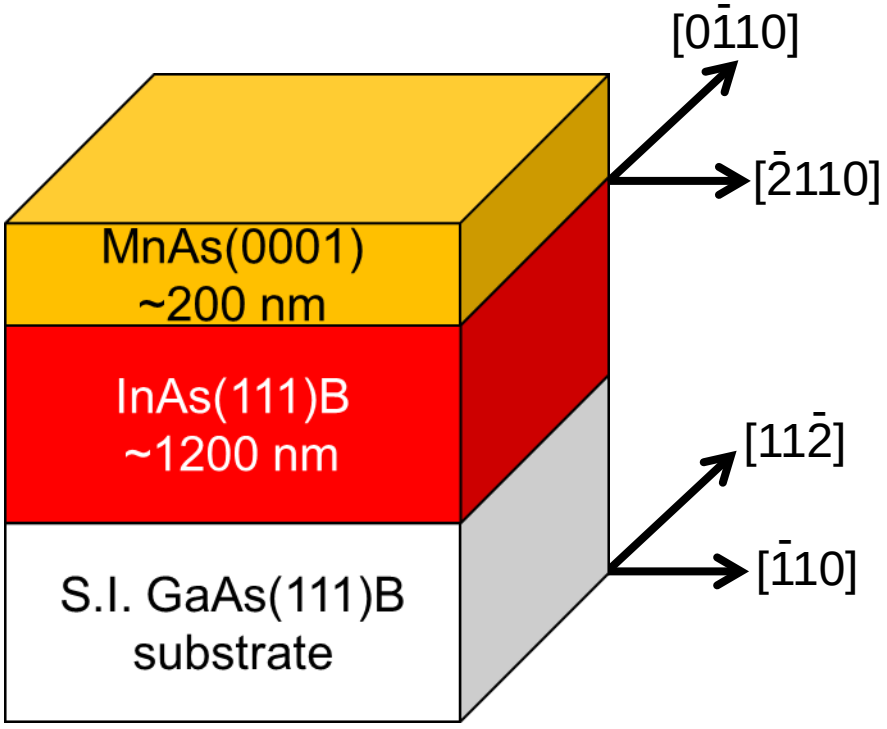

FIG. 1. Layer stacking of MnAs/InAs/GaAs.

To measure magnetic properties we cut the samples to 5 mm X 5 mm square chips, and then loaded the chips into a superconducting quantum interference device (SQUID) magnetometer.

To measure electrical properties we performed transmission line model (TLM) device fabrication using photolithography. First, we patterned MnAs electrodes by

photolithography, and then carried out wet chemical etching of MnAs using H_3PO_4:H_2O_2:H_2O = 3:1:200. The etching rates for MnAs and InAs were ~100 nm/min and ~20 nm/min, respectively. The electrode width and length were ~180 μm and ~90 μm, respectively. Next, we patterned InAs channels also by photolithography, and then carried out wet chemical etching of InAs by H_3PO_4:H_2O_2:H_2O = 3:1:50 with the etching rate of ~100 nm/min. The channel width was ~200 μm close to the electrode width, and the length (*L*) was varied between 20 μm and 70 μm. Figure 2(a) shows an optical microscope photograph of a fabricated TLM device, and significant side-etching behaviors in both MnAs and InAs can be seen. Therefore, the wet chemical etching is not suitable for precise MnAs electrode formation.

We also tried to fabricate lateral spin-valve (LSV) devices. With considering the side etching of MnAs as mentioned above, we used the combination of electron-beam lithography (EBL) and Ar^+ ion beam etching. Two electrode lengths of ~1 μm and ~3 μm were prepared to obtain different coercive magnetic fields for anti-parallel magnetization status. The electrode spacing (*L*) was varied between 1 μm and 3 μm. InAs channels were defined by EBL and wet chemical etching similar to TLM device fabrication with expanded resist patterns with considering the side etching of InAs. The channel width was designed ~20 μm. Figures 2(b) and (c) show an optical microscope photograph and a schematic of LSV device, respectively. Even though MnAs electrodes almost can be kept, however, the side

etching of InAs channel still can be seen due to underestimation of InAs side-etching.

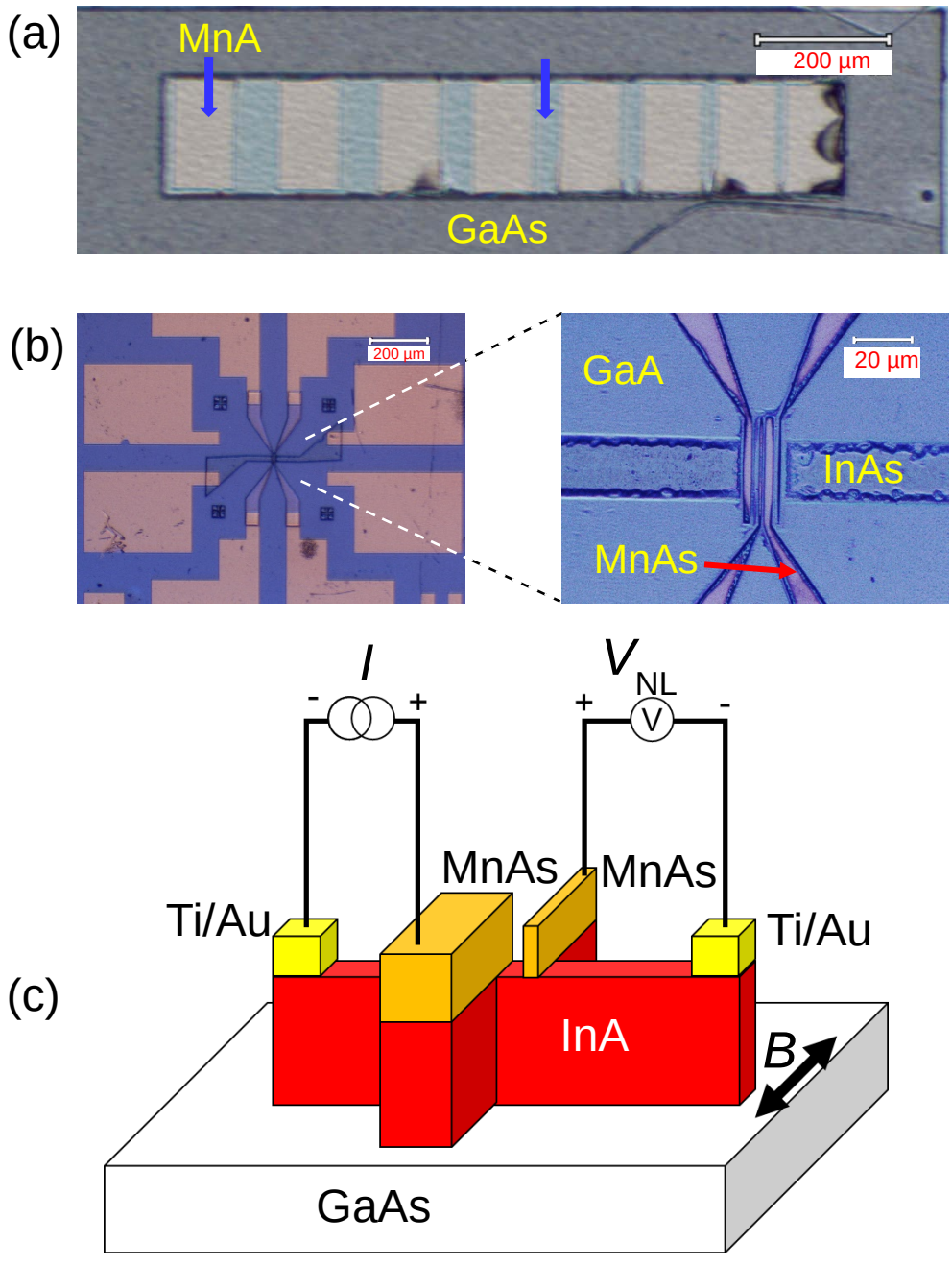

FIG. 2. Optical microscope photographs of (a) TLM device and (b) LSV

We could confirm the etching process is reproducible in TLM and LSV devices fabrication with significant side etching. Therefore, we need dry etching process to improve both MnAs electrode and InAs channel formations.

3. Magnetic properties

Figure 3 shows magnetization curves at 300 K as a function of applied magnetic field (H) parallel to two in-plane directions $[\bar{2}110]$ and $[0\bar{1}10]$ of hexagonal MnAs. We confirmed ferromagnetic behaviors at 300 K, and found easy and almost isotropic magnetization along in-plane directions which is similar to MnAs on GaAs(111)B [8]. The saturation magnetization (M_S) and the coercive field (H_C) are ~300 emu/cm^3 and ~320 Oe, respectively. Here, we have neglected diamagnetic influence of GaAs and InAs into the magnetization because of higher magnetic moment (~100 times) of ferromagnetic MnAs than diamagnetic GaAs and InAs of the sample.

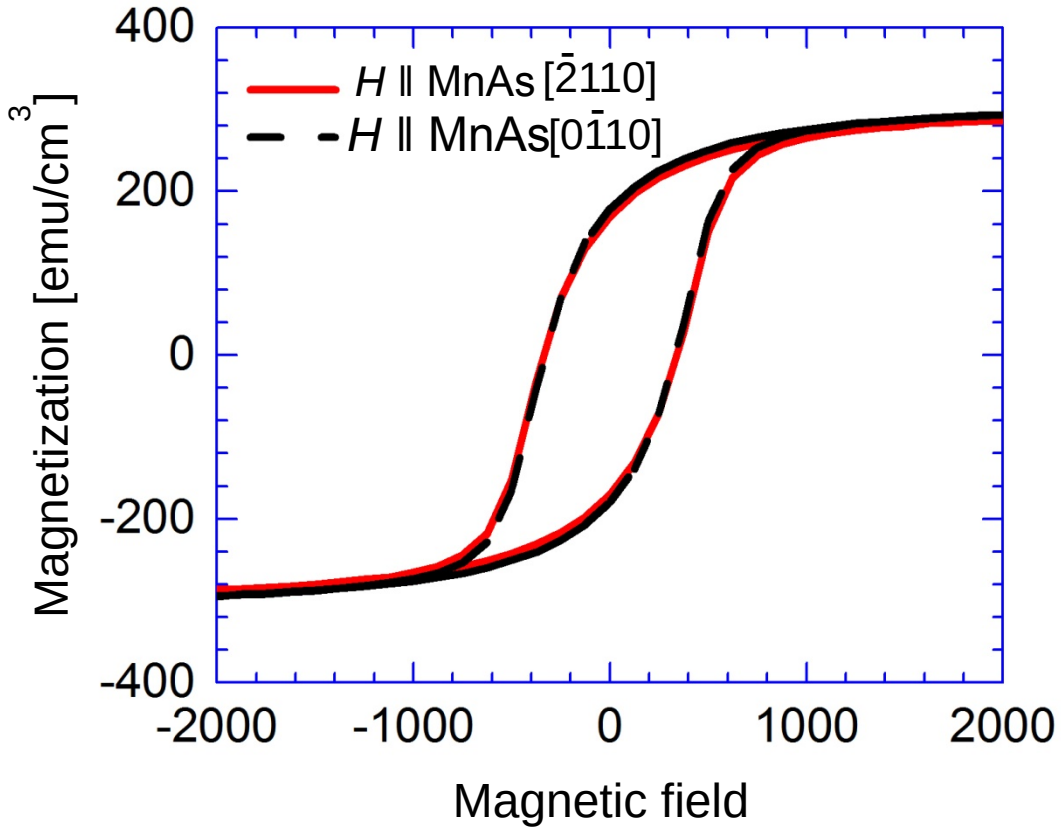

FIG. 3. Magnetization curves at 300 K of $[\bar{2}110]$ and $[0\bar{1}10]$ directions of hexagonal MnAs.

4. Electrical properties

Figures 4(a) and (b) show current (I)-voltage (V) characteristics of TLM devices with the channels along $[\bar{1}10]$ and $[11\bar{2}]$ of cubic InAs, respectively. Each curve seems almost linear. Therefore, we can conclude MnAs/InAs interface is Ohmic contact. Figure 5 shows their TLM plots. We found almost isotropic behaviors in two in-plane directions. The extracted electrical parameters, sheet resistance (R_S) of InAs channel, contact resistance (R_C) between MnAs/InAs and specific contact resistance (r_C) are summarized in Table 1. From the extracted data, we see almost no in-plane dependency of the basic electrical properties having little higher specific contact resistance of ~4 X 10^{-4} Ω-cm^2 through MnAs/InAs interface than typical Ohmic contact of III-V semiconductors [12]. We note that Hall effect of the hybrid structure indicates p-type conduction with sheet resistance of ~6.3 Ω/sq mainly from MnAs layer. In addition, from TLM measurements, we extracted InAs sheet resistance of ~950 Ω/sq, which is significantly higher than that of MnAs. Therefore, the MnAs/InAs interface can act as p^+/n^+ junction, which includes a tunnel barrier. The tunnel barrier may increase specific contact resistance.

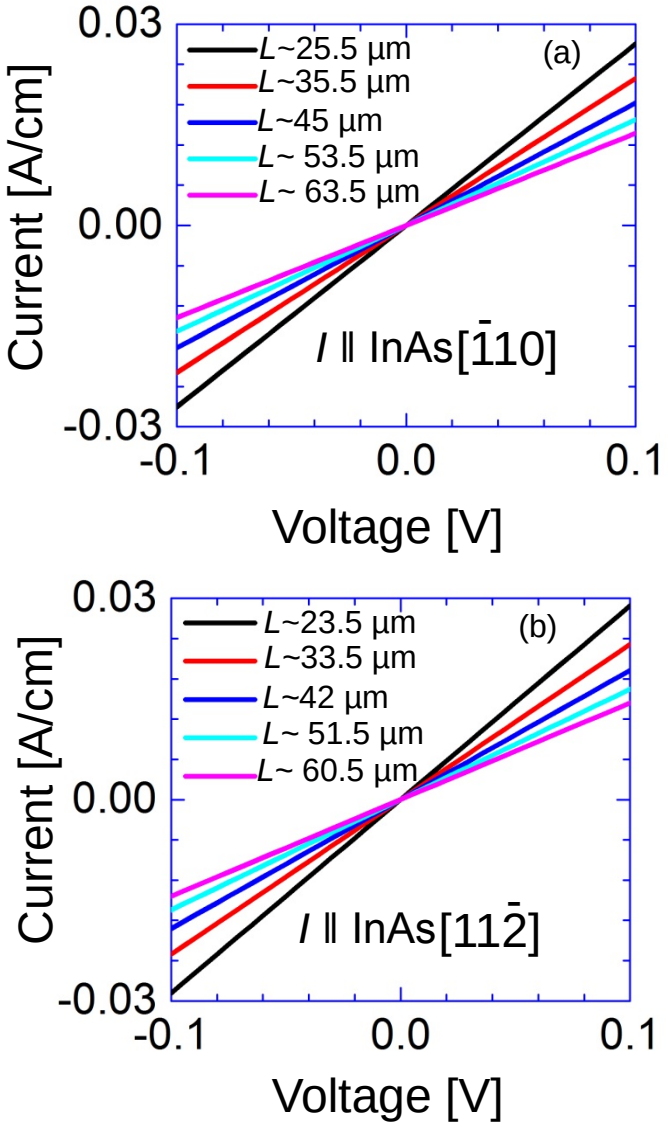

FIG. 4. Current-voltage characteristics of TLM devices with the channels along (a) $[\bar{1}10]$ and (b) $[11\bar{2}]$ of cubic InAs.

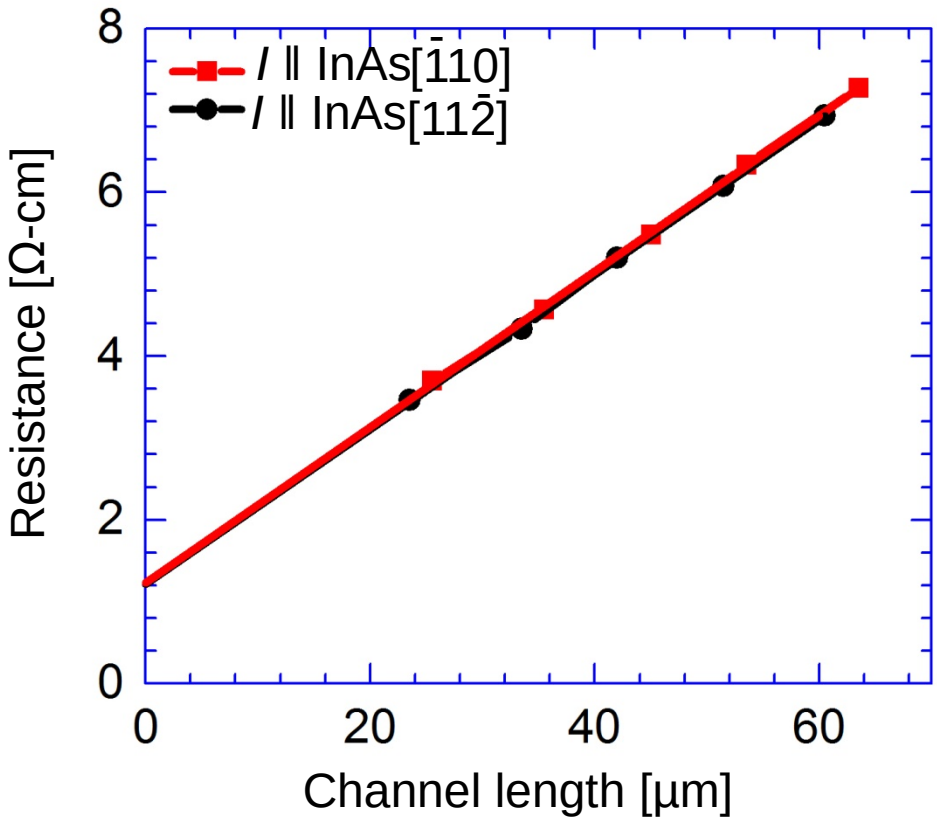

FIG. 5. TLM plots along $[\bar{1}10]$ and $[11\bar{2}]$ of cubic InAs.

Table 1 Electrical properties from TLM plots.

In-plane direction	R_S [Ω/sq.]	R_C [Ω-cm]	$L_t = R_C / R_S$ [μm]	$r_C = (R_C)^2 / R_S$ [Ω-cm^2]
$[\bar{1}10]$	950	0.61	6.42	4.3 X 10^{-4}
$[11\bar{2}]$	945	0.60	6.34	4.2 X 10^{-4}

5. Spin-valve measurements

Figure 6 shows non-local SV signal curves in MnAs electrode spacing of 1 μm along $[11\bar{2}]$ direction at room temperature. The signal does not seem so clear, however, SV like dips with hysteresis can be found around +25 and -15 mT. The asymmetric dips to zero magnetic field might be caused by hysteresis of magnet system. The dips in principal correspond to anti-parallel status, and we confirmed anti-parallel could be realized around several 10's mT by magnetic force microscopy using a patterned MnAs sample with similar configuration. We also checked electrode spacing dependence as shown in Fig. 7, and roughly obtained

the spin injection efficiency (P_i) of ~8.5% and the spin diffusion length (L_S) of ~0.7 μm. The values seem hopeful compared with values in ex-situ-formed CoFe/InGaAs [13], however, we note that there are some problems in device fabrication like etchant penetration and in data reliability like asymmetric behavior of spin-valve signal curves to zero magnetic field.

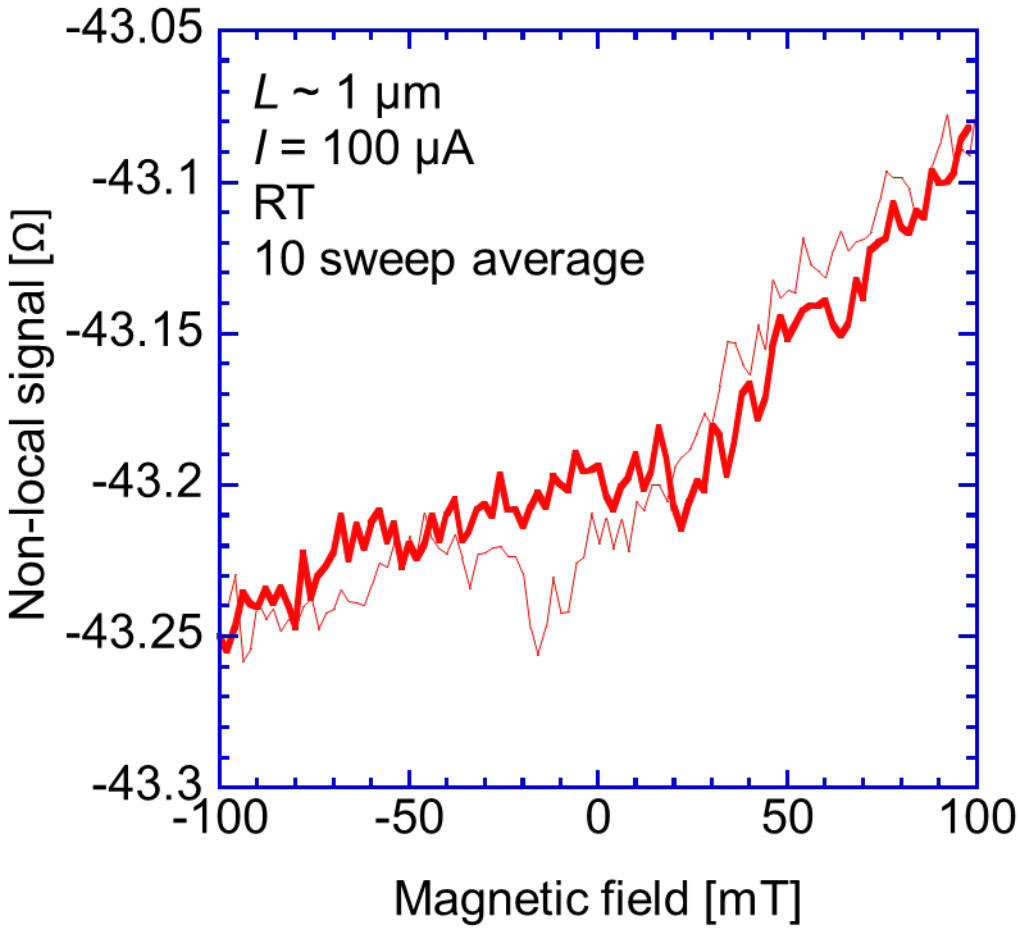

FIG. 6. Non-local SV signal curves in MnAs electrode spacing of 1 μm along[$11\bar{2}$] direction at room temperature.

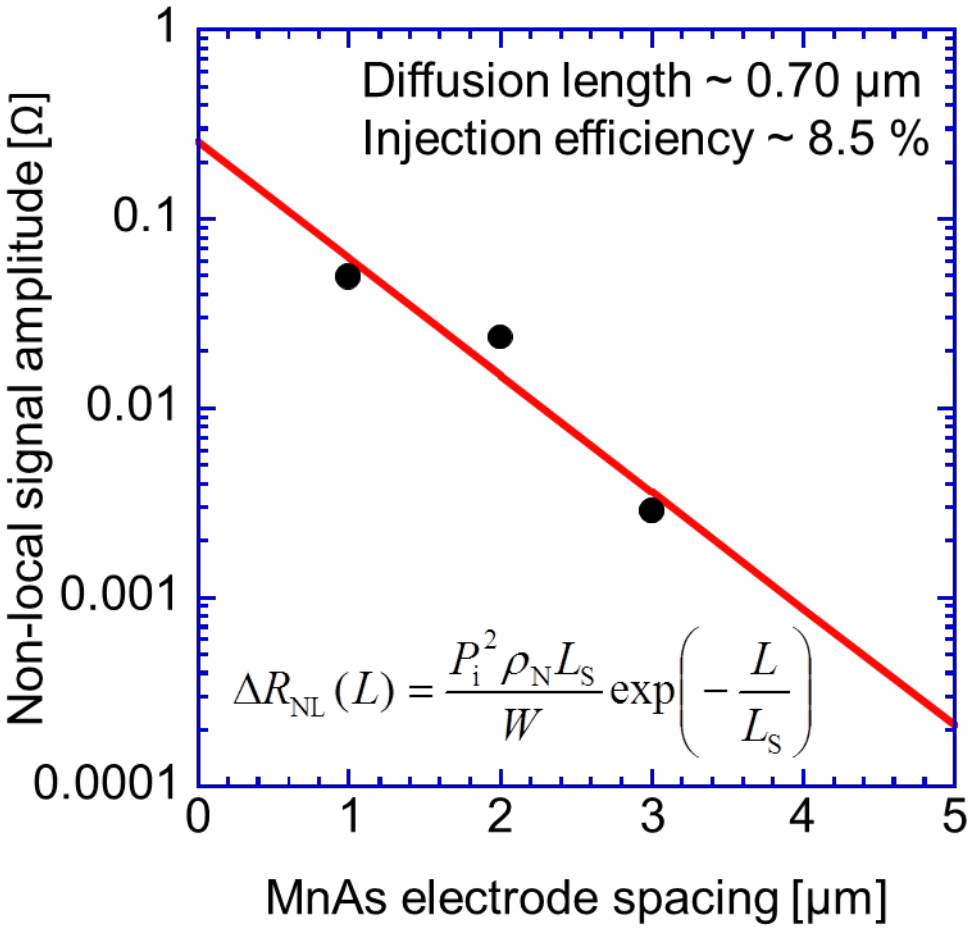

FIG. 7. Electrode spacing dependence of SV signal amplitude.

6. Conclusion

We confirmed isotropic in-plane magnetization and isotropic basic electrical properties of MnAs/InAs/GaAs(111)B hybrid structure grown by MBE. M_S and H_C at 300 K are ~300 emu/cm^3 and ~320 Oe, respectively. r_C of MnAs/InAs interface at room temperature is ~4 X 10^{-4} Ωcm^2. Also we tried to fabricate and characterize LSV devices. We roughly obtained the spin injection efficiency of ~8.5% and the spin diffusion length of ~0.7 μm at room temperature. We believe that the hybrid structures are helpful to design spintronic device with good flexibility in-plane.

Acknowledgement

This work was supported by The Murata Science Foundation 2016 in part.

References

[1] S. Datta and B. Das: Appl. Phys. Lett. 56 (1990) 665.

[2] J. B. Goodenough and J. A. Kafalas*:* Phys. Rev. 157 (1967) 389.

[3] M. Tanaka, J. P. Harbison, M. C. Park, Y. S. Park, T. Shin, and G. M. Rothberg: Appl. Phys. Lett. 65 (1994) 1964.

[4] M. Tanaka, J. P. Harbison, M. C. Park, Y. S. Park, T. Shin, and G. M. Rothberg: J. Appl. Phys. 76 (1994) 6278.

[5] M. Yokoyama, S. Ohya, and M. Tanaka: Appl. Phys. Lett. 88 (2006) 012504.

[6] Y. Morishita, K. Iida, J. Abe, and K. Sato: Jpn. J. Appl. Phys. 36 (1997) L1100.

[7] S. Hara and T. Fukui: Appl. Phys. Lett. 89 (2006) 113111.

[8] L. B. Steren, J. Milano, V. Garcia, M. Marangolo, M. Eddrief, and V. H. Etgens: Phys. Rev. B 74 (2006) 144402.

[9] D. Saha, M. Holub, P. Bhattacharya, and Y. C. Liao: Appl. Phys. Lett. 89 (2006) 142504.

[10] H. Kum, D. Basu, P. Bhattacharya, and W. Guo: Appl. Phys. Lett. 95 (2009) 212503.

[11] E. Islam and M. Akabori: J. Cryst. Growth 463 (2017) 86.

[12] A.G Baca, F Ren, J.C Zolper, R.D Briggs, and S.J Pearton: Thin Solid Films 308 (1997) 599.

[13] S. Hidaka, M. Akabori, and S. Yamada: Appl. Phys. Express 5 (2012) 113001.